

Interdiffusion Studies between a Mo-Based Alloy and Ti

A. LAIK, G.B. KALE, and K. BHANUMURTHY

Interdiffusion between Ti and a Mo alloy (TZM) has been studied in the temperature range of 1273 to 1373 K. Boltzmann–Matano and Hall’s methods were used to evaluate the interdiffusion coefficients. The microstructure of the TZM/Ti interface showed excellent contact for all specimens bonded above 1273 K. The reaction index (n) evaluated by layer growth kinetics was close to 2. Interdiffusion coefficients increase with the increase in Ti concentration, and a quadratic relationship could be determined between the activation energy and concentration of Ti. Impurity diffusion coefficients of Mo in Ti and the activation energy for diffusion of Mo in Ti were evaluated. A linear dependence between the activation energy (Q) and pre-exponential factor (D_0) for interdiffusion could be established. The diffusion parameters for TZM/Ti in the present studies were also compared with the earlier work on the Mo/Ti system and there seems to be a good correlation between these two studies.

I. INTRODUCTION

IN a tokamak fusion reactor, the diverter plates are made of carbon-fiber composites and tungsten and Mo-based alloy tubes are used as coolant tubes.^[1] Several designs use He-cooled structures with a nominal coolant temperature of 1173 to 1273 K.^[2] Operation of these reactors at such high temperatures requires refractory alloys with excellent high-temperature strength along with high thermal conductivity. Although Mo-based alloys show such properties, fabrication of structural components would require joining of these alloys. Due to the high thermal stresses generated during operation, coupled with the limited ductility of refractory alloys in general, joining by fusion welding is a poor choice. Solid-state diffusion bonding, on the other hand, is known for producing strong metallurgical bonds with less defects and better strength. Since the recrystallization temperature of refractory metals and alloys is very high, direct bonding would require very high temperatures throughout the furnace under vacuum, which is both difficult to achieve and uneconomical. The bonding temperature can be lowered to a large extent by using interlayers of reactive metals that have high solubility and do not form any brittle intermediate phase.

Among the Mo-based alloys used commercially, the most important and widely used alloy is TZM (Mo-0.5 pct Ti-0.08 pct Zr-0.05 pct C). This alloy is designated as molybdenum alloy 363 and molybdenum alloy 364 (ASTM standard ASTM B386-91). Due to its constituent elements, titanium (Ti), zirconium (Zr), and molybdenum (Mo), the alloy is popularly known as TZM. The alloy will be referred to as TZM henceforth in this article. The interdiffusion studies on the TZM-Ti system are not reported in the literature. However, some studies on the binary system of Ti-Mo are reported,^[3,4] but there seems to be some inconsistency in the values of the diffusion coefficients evaluated. Whereas the diffusion studies were performed in the temperature range 1199 to 1518 K, by Kale and Patil,^[3] those reported

by Thibon *et al.*^[4] were performed at a higher temperature range of 1573 to 1873 K. The interdiffusion coefficients evaluated by Kale *et al.*^[3] at 1518 K and by Thibon *et al.*^[4] at 1523 K vary by three orders of magnitude at 90 at. pct Mo composition. However, the composition dependence of the interdiffusion coefficient showed a similar trend in both these studies. Kale and Patil^[3] have shown that the activation energy Q and the pre-exponential factor D_0 increase with the increase in Mo concentration, whereas in the study by Thibon *et al.*,^[4] both Q and D_0 decrease with the increase in Mo concentration, with a local maxima at 30 at. pct Mo.

The present work deals with the study of the diffusion behavior of the TZM-Ti system. Interdiffusion coefficients and their composition and temperature dependence are determined by employing “sandwich”-type diffusion couples of bulk TZM and Ti in the form of foils as interlayers.

II. EXPERIMENTAL PROCEDURE

The present studies involve several steps such as the preparation of a sandwich type of diffusion couple, diffusion annealing, establishing the true concentration penetration profiles across the diffusion zone, and evaluation of the diffusion coefficients.

A. Preparation of Diffusion Couples

Sandwich-type diffusion couples were made with TZM and Ti (99.9 pct) foils. Cylindrical pieces of TZM of 12.5-mm diameter and 4-mm height and Ti foil of 200- μ m thickness were used to make the diffusion couples. The surfaces of the TZM pieces were prepared by grinding on successive grades of emery paper starting from 120 through 600 grit and finally polished on a lapping wheel with diamond paste of 1 μ m. The pieces were loaded on a vacuum hot press keeping the Ti sheet between the two TZM pieces. Mica sheets were used on the top and bottom surfaces of the diffusion couples to prevent diffusion of carbon from the graphite rams to the diffusion couples. A uniaxial compressive pressure of 5 MPa was applied and the couple was heated at 1273 K for 0.25 hours for intimate contact and thereafter furnace cooled to minimize the residual stresses at the interface.

A. LAIK, Scientific Officer, G.B. KALE and K. BHANUMURTHY, Group Leaders, Diffusion and EPMA Group, are with the Materials Science Division, Bhabha Atomic Research Center, Mumbai - 400 085, India. Contact e-mail: laik@barc.gov.in

Manuscript submitted February 17, 2006.

B. Diffusion Annealing

The diffusion couples were then encapsulated in quartz capsules in He atmosphere at a residual pressure of 150 mbar for further heat treatment. The encapsulated samples were diffusion annealed in a resistance heating horizontal furnace for various time intervals at different temperatures. The temperature of the furnace was kept constant within ± 1 K using a proportional type of temperature controller. The details of the heat treatment schedule are given in Table I. After the heat treatment, the capsules were quenched in water.

C. Metallographic Preparation

Cross sections of the couples were taken using a low speed diamond saw parallel to the diffusion direction. The cross sections of the couples were prepared for further electron-optical analysis using the standard metallographic techniques. The polished surfaces of the couples were etched with an etchant (lactic acid: HNO_3 : HF = 6:2:1 by volume) to reveal the microstructure of the annealed couples. The microstructures of the etched diffusion couples were recorded using an optical microscope.

D. Electron Probe Microanalysis

A Cameca SX100 electron probe microanalyzer (EPMA) equipped with a three-wavelength dispersive spectrometer was used to analyze the diffusion couples. A well-focused stabilized electron beam of 20 kV voltage and 20 nA current was used for analysis. Lithium fluoride (LiF) crystal was used for diffraction of $\text{Ti } K_\alpha$, and pentaerythritol (PET) crystal was used for $\text{Mo } L_\alpha$ and $\text{Zr } L_\alpha$. Quantitative analysis of the samples was done on a point-to-point basis at intervals of 1 to 2 μm across the diffusion zone to determine the concentration profile. Pure elemental standards of Ti, Mo, and Zr were used for calibration of the equipment. Standard PAP correction^[5] was used to arrive at a concentration from the intensity ratio values. After the diffusion bonding, the interface of the couples was analyzed using a EPMA. It was observed that the width of the diffusion zone for the as-bonded specimens (1273 K for 0.25 hours) was very small compared to the diffusion width of the diffusion couples annealed subsequently and hence was neglected for further analysis.

III. RESULTS AND DISCUSSION

A. Microstructures

The optical microstructure of the longitudinal section of the cylindrical pieces of TZM used for making the diffusion

Table I. Heat Treatment Schedule for the Diffusion Annealing of the Diffusion Couples

Couple	Temperature (K)	Time (h)
1	1273	2
2	1273	4
3	1273	10
4	1323	4
5	1373	4

couples is shown in Figure 1. The microstructure consists of large elongated grains of about 150 to 250 μm in length and 40 to 60 μm in width. The elongated grains are essentially due to the thermomechanical process the material has experienced. Small precipitates of carbides are found all along the grain boundaries. X-ray mapping of Ti, Mo, Zr, and C confirmed these precipitates to be essentially rich in Ti and C.

Figure 2 shows a backscattered electron image of the diffusion couple annealed at 1323 K for 4 hours. A 200- μm -thick Ti foil can be seen between the TZM pieces on either side. The microstructure shows that the diffusion zone has nearly uniform thickness throughout and is planar in morphology. Fine needle-shaped structures seen in the central portion of the Ti foil are of α' -Ti. These are formed due to martensitic transformation of β -Ti phase while quenching in water after the diffusion annealing. The α' plates of martensite are formed only on the central part

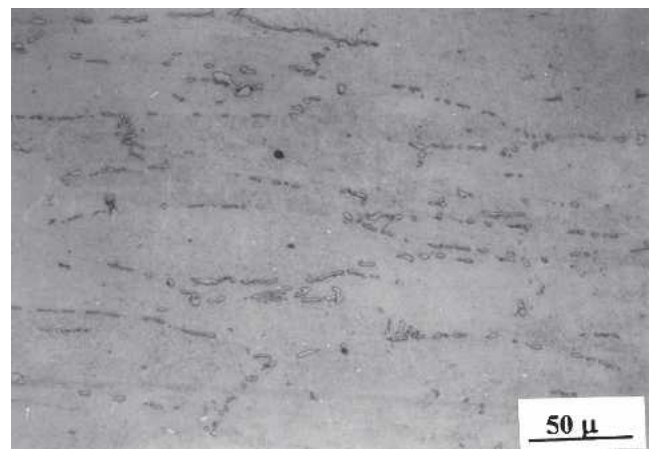


Fig. 1—Optical micrograph of TZM showing the elongated grains and carbide precipitates along the grain boundaries.

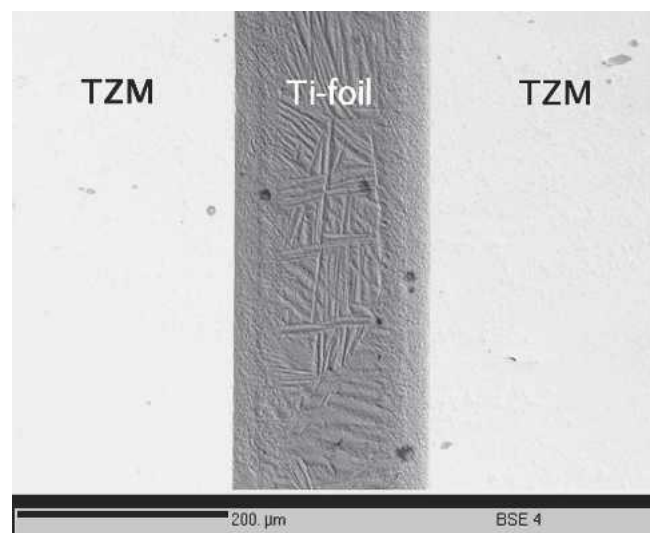


Fig. 2—Backscattered electron micrograph of the diffusion couples annealed at 1323 K for 4 h. The Ti foil appears between the TZM blocks.

of the Ti foil, which remains unaffected by the diffusion of Mo into Ti. Because Mo is a β stabilizer, it stabilizes the β phase of the diffusion zone about 50 μm on each side. The variation in the chemistry across the Ti foil is shown by the intensity profile of Ti, Mo, and Zr in Figure 3.

The bonding between TZM and Ti was found to be excellent on both the sides of Ti. The TZM-Ti interfaces in all the diffusion couples were sound. Any type of cracks or discontinuity could not be detected at the interface. However, specimens bonded at lower temperatures (<1273 K), during some preliminary experiments, did show the presence of pores, indicating the absence of bonding. In view of this, the bonding was carried out at 1273 K for 0.25 hours.

B. Concentration Profiles

A typical concentration profile of Ti, Zr, and Mo across the TZM-Ti interface of the couple annealed at 1273 K for 4 hours is shown in Figure 4. The nature of these profiles for other couples was found to be nearly the same. These concentration penetration profiles in all the samples are solid solution type in nature.

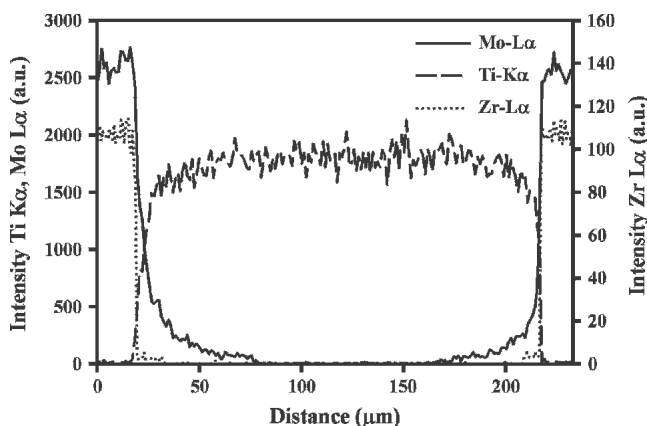


Fig. 3—Intensity profiles of Mo L_{α} , Zr L_{α} , and Ti K_{α} X-rays across the TZM/Ti/TZM diffusion couple annealed at 1323 K for 4 h.

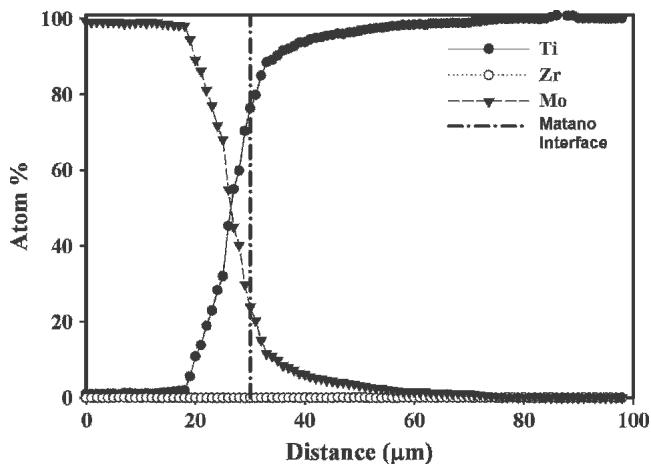


Fig. 4—Concentration profile across the interface of the couple annealed at 1273 K for 4 h.

It is very clear from these profiles that Mo diffuses much deeper into Ti than Ti diffuses into Mo. A marked asymmetry is noticed in the concentration profile about the Matano interface. The diffusion width ranges from 50 to 80 μm . The concentration of Mo changes from 99 to 10 pct within only 10 pct of the diffusion zone, beyond which the concentration of Mo changes very gradually to zero and extends deep into Ti. This asymmetry is due to the difference in the intrinsic diffusion coefficients of Ti and Mo. It can be inferred from the concentration profiles that the intrinsic diffusivity of Ti is much higher than that of Mo in the present range of temperature. The variation in the concentration of Zr and C is negligible and the profile is nearly flat. Hence, it can be assumed that the influence of Zr and C is almost negligible in the interdiffusion of TZM and Ti. The present system, therefore, can be treated as a pseudo-binary system of Mo and Ti.

C. Kinetics of Diffusion

The widths of the diffusion zones were determined from the concentration profiles for all the couples. The kinetics of growth of the diffusion zone with annealing time can be estimated by plotting the width of the diffusion zone against time of annealing on a log-log scale. The growth of the diffusion zone, in general, is expressed as

$$w = kt^{1/n} \quad [1]$$

where w is the width of the diffusion zone and t is the time of annealing. The parameters k and n describe the kinetics and are called the penetration constant and reaction index, respectively.

Figure 5 shows a plot of $\ln w$ vs $\ln t$. The least-squares method was used for fitting a straight line to these data points. The values of $n = 1.988$ and $k = 4.2955 \times 10^{-7} \text{ ms}^{-0.503}$ were calculated from the slope and intercept of the straight line, respectively. For an ideal diffusion-controlled process, the value of $n = 2$, and the value of n determined based on present experiments is close to 2. Hence, it may be assumed that the present process is essentially diffusion controlled.

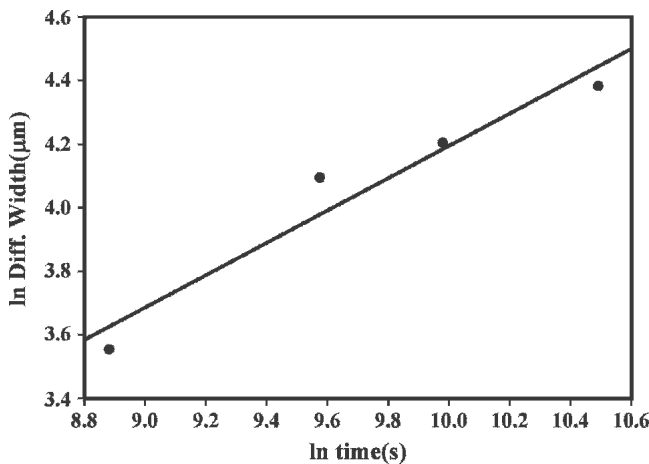


Fig. 5—Diffusion widths plotted against the time of annealing in logarithmic scale.

D. Evaluation of Interdiffusion Coefficients

The concentration-dependent interdiffusion coefficient $\tilde{D}(C)$ in a binary system can be evaluated using the Boltzmann–Matano method.^[6,7] The interdiffusion coefficient \tilde{D} at composition C^* is given by

$$\tilde{D}(C^*) = -\frac{1}{2t} \left(\frac{dx}{dC} \right)_{C^*} \int_{C=C^{-\infty}}^{C=C^*} (x - x_0) dC \quad [2]$$

where $\left(\frac{dx}{dC} \right)_{C^*}$ is the inverse of the concentration gradient at C^* ; $C^{-\infty}$ and $C^{+\infty}$ are the concentration at $x = -\infty$ and $x = +\infty$, respectively (*i.e.*, at infinite distance from the diffusion zone), and x_0 is the coordinate of the Matano interface (MI). The initial condition for Eq. [2] is

$$\text{at } t = 0, \quad C = C^{-\infty}; \quad x < x_0$$

$$C = C^{+\infty}; \quad x > x_0.$$

The position of the MI is determined from the condition

$$\int_{C^{-\infty}}^{C^{+\infty}} x dC = 0. \quad [3]$$

The interdiffusion coefficients, \tilde{D} , were evaluated for all of the temperatures of annealing at an interval of 10 at. pct concentration using the Boltzmann–Matano method. The values of \tilde{D} determined in the current study are about an order of magnitude lower than those reported by Kale and Patil^[3] in the same range of annealing temperatures.

E. Composition Dependence of Interdiffusion Coefficients

The interdiffusion coefficient \tilde{D} increases with the increase in the concentration of Ti (Figure 6). The linear

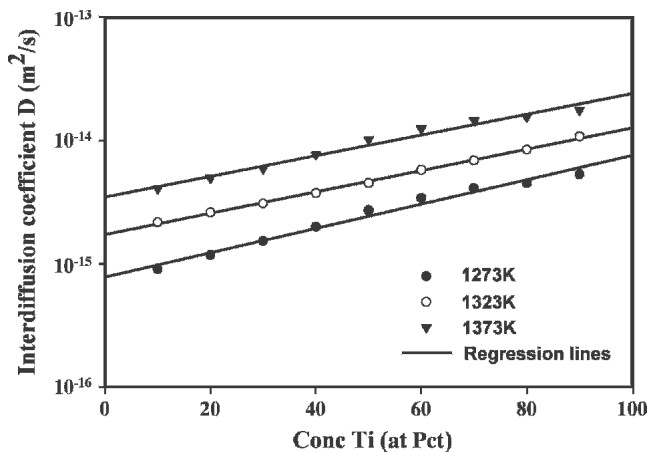


Fig. 6—Concentration dependence of the interdiffusion coefficient at all the temperatures of annealing.

variation is very evident. Therefore, the values of $\ln \tilde{D}$ were fitted to C_{Ti} by linear regression for each temperature of annealing. The concentration dependence of \tilde{D} can thus be expressed as

$$\ln \tilde{D} = a + bC_{Ti}. \quad [4]$$

Here, the values of \tilde{D} are expressed in m^2/s and those of C_{Ti} are expressed in at. pct. The values of the constants a and b at each temperature of annealing were calculated from the linear relations and are presented in Table II. Such linear relations were also reported in earlier work in the Ti–Mo system.^[3,4] Thibon *et al.*,^[4] however, had reported that at 1523 K, there is a strong dependence of the interdiffusivity, \tilde{D} , with the composition. The interdiffusion coefficients vary as much as 3×10^3 times between the concentration limits (1 and 99 at. pct Mo). In the current study, as well as that reported by Kale and Patil,^[3] \tilde{D} varies within one order of magnitude even at the highest temperature of annealing (1373 K).

In a binary system, the interdiffusion coefficient \tilde{D} can be related to the melting point or the solidus temperature. It is related to the ratio T/T_m , where T is the temperature of annealing and T_m is the melting temperature or the solidus temperature. Hence, \tilde{D} can be related to the composition. Le Claire^[8] has shown that the increase in the concentration of the solute leads to an increase in \tilde{D} if it is accompanied by a decrease in the melting point in the solvent and *vice versa*. In the present system of Ti–Mo, the solidus line shows a monotonic decrease with increasing concentration of Ti. Hence, one should expect a continuous increase in the \tilde{D} values with an increase in C_{Ti} , and the values are in accordance with Le Claire's analysis.^[8]

F. Temperature Dependence of Interdiffusion Coefficients

The interdiffusion coefficient \tilde{D} follows an Arrhenius relation:

$$\tilde{D} = \tilde{D}_0 \exp(-Q/RT). \quad [5]$$

To determine the activation energy for interdiffusion, Q , and the pre-exponential factor, \tilde{D}_0 , the $\ln \tilde{D}$ values were plotted against the reciprocal of temperature of annealing for different compositions at an interval of 10 at. pct (Figure 7). The data points for each concentration were fitted with linear relation using the least-squares method. The values of Q and \tilde{D}_0 were determined from the slope and intercept of the straight lines and are shown in Table III. The values of Q range from 174.4 to 218.5 kJ/mol, and the values of \tilde{D}_0 range from 8.7×10^{-7} to $7.9 \times 10^{-8} m^2/s$. The values of the activation energy determined by Kale and

Table II. Values of the Constants a and b for the Relation $\ln \tilde{D} = a + bC_{Ti}$ (Equation [4])

Temperature (K)	a	b
1273	−34.783	0.0227
1323	−33.989	0.0199
1373	−33.283	0.0193

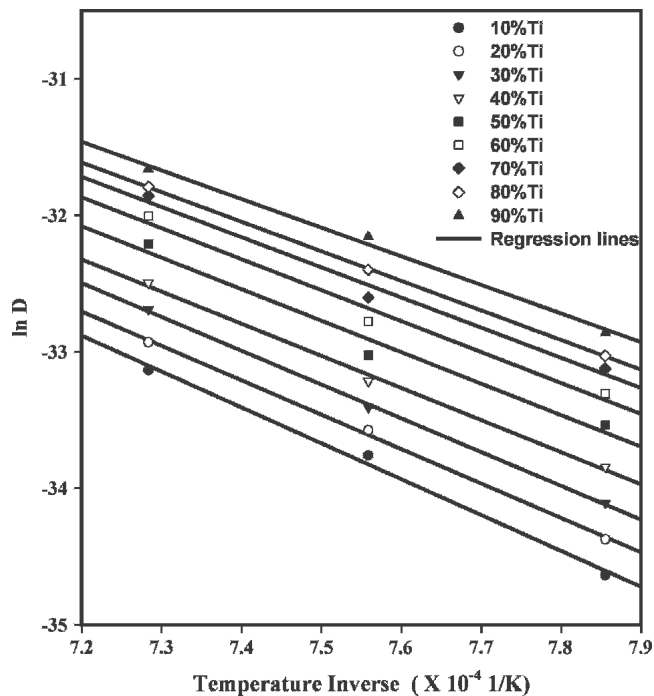


Fig. 7—Temperature dependence of the interdiffusion coefficients at 10 at. pct interval of Ti concentration.

Table III. Activation Energy (Q) and Pre-Exponential Factor (D_0) for Interdiffusion at Various Compositions; the Activation Energy Values are Compared with Other Reported Works on the Mo-Ti System

C_{Ti} (At. Pct)	D_0 ($\times 10^{-7} \text{ m}^2/\text{s}$)	Q (kJ/mol)	$Q^{[3]}$ (kJ/mol)	$Q^{[9]}$ (kJ/mol)
10	8.67	218.5	207.2	196.6
20	4.90	209.9	194.5	196.6
30	4.24	205.8	192.5	209.2
40	2.08	195.6	185.2	217.6
50	1.94	191.9	179.1	234.3
60	1.79	188.6	177.5	255.2
70	1.36	183.6	168.9	263.6
80	1.09	179.9	148.7	217.6
90	0.79	174.4	152.8	219.2

Patil^[3] in their study in the temperature range of 1199 to 1518 K and those determined in a study at higher temperature range (1573 to 1873 K)^[9] are also listed in Table III for comparison. The range of the values of Q determined in the current study matches well with the values reported in both these studies. The values of Q were found to decrease with the increase in the Ti concentration. Kale and Patil^[3] have also reported such observations, whereas those reported by Gurney^[9] show a reverse trend. The interdiffusion study by Thibon *et al.*^[4] in the same binary system of Mo-Ti has shown that the activation energy Q increases to about 280 kJ/mol for 70 pct Ti and thereafter decreases to about 250 kJ/mol for Ti concentration of 95 pct. The pre-exponential factor, D_0 , also decreases with an increase in the concentration of Ti in the Mo-Ti system.

Since the activation energy for interdiffusion (Q) and the pre-exponential factor (D_0) are found to vary systematically

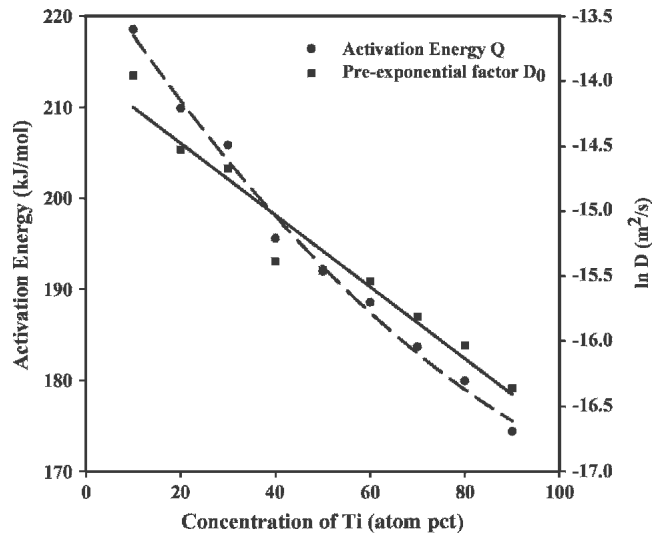


Fig. 8—Composition dependence of pre-exponential factor (D_0) and activation energy (Q) for interdiffusion.

with the composition, it was attempted to express these parameters by mathematical relationships. In Figure 8, both the parameters were plotted against the Ti concentration. The Q values are in linear scale, whereas the D_0 values are in logarithmic scale. The values of $\ln D_0$ decrease linearly with an increase in C_{Ti} . A linear relation could be fitted to the $\ln D_0$ values by linear regression and can be expressed as

$$\ln D_0 = -13.264 - 2.7566 \times 10^{-2} C_{Ti}, \quad [6]$$

where the values of D_0 are expressed in m^2/s and those of C_{Ti} are expressed in at. pct.

The variation in the activation energy values with the Ti concentration is not linear, on the other hand. The slope of Q in Figure 8 is higher at a lower concentration of Ti than at higher concentrations. Therefore, a quadratic relation was established between Q and C_{Ti} with a correlation factor of 0.99166. The relation is expressed as

$$Q = 225.6 - 0.7934 C_{Ti} + 2.642 \times 10^{-3} C_{Ti}^2, \quad [7]$$

where the values of Q are expressed in kJ/mol and those of C_{Ti} are expressed in at. pct. Kale and Patil^[3] had reported a linear variation of Q with C_{Ti} .

By combining Eqs. [6] and [7], one can obtain a single relation, which gives both the composition and the temperature dependence of the interdiffusion coefficient \tilde{D} (in kJ/mol):

$$\begin{aligned} \tilde{D} = & 5.76 \times 10^{-5} \exp(-2.7566 \times 10^{-2} C_{Ti}) \\ & \times \exp[-(225.6 - 0.7934 C_{Ti} + 2.642 \times 10^{-3} C_{Ti}^2)/RT]. \end{aligned} \quad [8]$$

G. Impurity Diffusion Coefficient

The Boltzmann–Matano method involves numerical solution to the Fick's laws by estimating the slope of the

concentration profile and the area covered under the curve. The diffusion coefficients calculated by using this method at the ends, therefore, do not result in accurate values. In such a situation, one can employ Hall's method^[10] (an analytical method) to arrive at sufficiently accurate results at the end of the profile.

A variable, λ , is defined as

$$\frac{C}{C_0} = \frac{1}{2}(1 + \operatorname{erf}(\lambda)), \quad [9]$$

where C is the solute concentration at position x with respect to the Matano interface after an annealing of time interval t , $C_0 = |C^{+\infty} - C^{-\infty}|$, and $\operatorname{erf}(\lambda)$ is an error function of λ . Both λ and $\eta(=x/\sqrt{t})$ are found to hold a linear relationship:

$$\lambda = h\eta + k. \quad [10]$$

The values of h and k are determined from the slope and intercept of the straight-line fit to the plot of λ vs η . The concentration-dependent interdiffusion coefficient \tilde{D} at concentration (C^*) can be determined by the following relation:

$$\tilde{D}(C^*) = \frac{1}{4h^2} + \frac{k\sqrt{\pi}}{4h^2}(1 + \operatorname{erf}(\lambda)) \exp(\lambda^2). \quad [11]$$

Figure 9 shows the plot of λ vs η for the couple annealed at 1273 K for 4 hours. The interdiffusion coefficient values \tilde{D} were evaluated for all the temperatures of annealing in the Ti side, *i.e.*, concentration range 0 to 10 at. pct Mo. A typical plot of $\tilde{D}(C^*)$ against C_{Mo} is shown in Figure 10 for the diffusion couple annealed at 1273 K for 4 hours. In the terminal solid solution regime, the \tilde{D} varies almost linearly with C_{Mo} (Figure 10). A linear relation was fitted through all the points for each plot and extrapolated to infinite dilution, *i.e.*, $C_{\text{Mo}} \rightarrow 0$. This gives the impurity diffusivity of Mo in Ti, $D_{\text{Mo}}^{\text{Ti}}$. Askill and Gibbs^[11] have calculated the impurity diffusivity of the isotope Mo^{99} in Ti by the radio-tracer method. Onodera *et al.*^[12] have also reported the impurity diffusion coefficient of Mo in Ti. Thibon *et al.*^[4] had determined the values of impurity diffusion coefficient of Mo in Ti using the Hall's method in the temperature range 1523 to 1873 K. Since the temperature range in which all these values are reported does not match exactly with the range of present studies, these values are fitted to Arrhenius relations and then extrapolated to the present temperature range. The impurity diffusion coefficients determined at various temperatures are shown in Table IV along with those calculated from other reported values. It can be

noticed that the values evaluated in the current study match well with those determined by Askill and Gibbs,^[11] Onodera *et al.*,^[12] and Thibon *et al.*^[4] (Table IV). The values of $D_{\text{Mo}}^{\text{Ti}}$ are fitted to an Arrhenius plot in Figure 11. The Arrhenius plots from other works are also traced in Figure 11, for comparison. It can be seen that the results from the present calculations match very well with those from the literature. The activation energy Q and the pre-exponential factor D_0 for the impurity diffusion coefficient of Mo in Ti were determined from the slope and intercept of the plot in Figure 11. The values are $Q = 171.98$ kJ/mol and $D_0 = 3.248 \times 10^{-7}$ m²/s. These values are close to the Q and D_0 values determined from the impurity diffusion of the

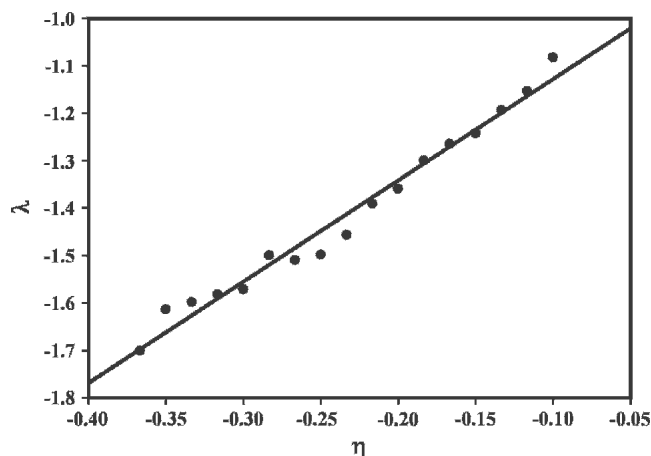


Fig. 9—The plot of λ vs η for the diffusion couple annealed at 1273 K for 4 h.

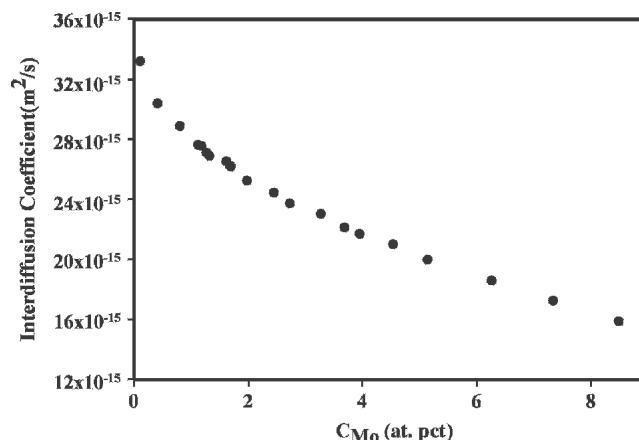


Fig. 10—Concentration dependence of the interdiffusion coefficient calculated using Hall's method.

Table IV. Impurity Diffusivity Values of Mo in Ti ($D_{\text{Mo}}^{\text{Ti}}$) at Various Temperatures

Temperature (K)	Present Study ($\times 10^{-14}$ m ² /s)	Askill and Gibbs ^[11] ($\times 10^{-14}$ m ² /s)	Onodera <i>et al.</i> ^[12] ($\times 10^{-14}$ m ² /s)	Thibon <i>et al.</i> ^[4] ($\times 10^{-14}$ m ² /s)
1273	3.011	1.733	3.234	9.775
1323	4.697	3.753	6.543	18.201
1373	9.839	7.681	12.571	32.405

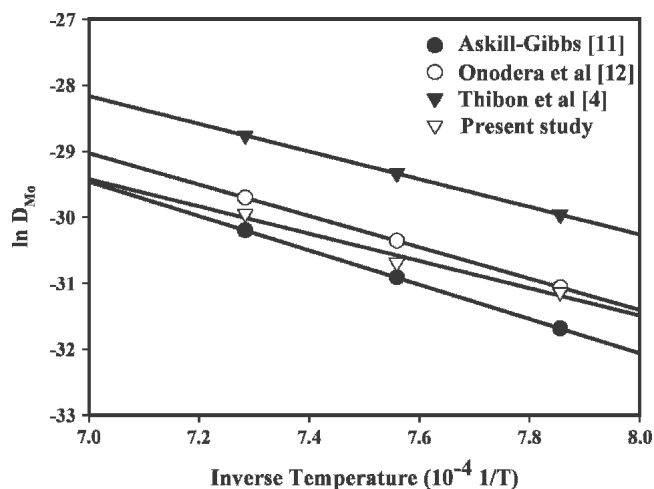


Fig. 11—Temperature dependence of impurity diffusivity of Mo in Ti.

Mo⁹⁹ isotope tracer.^[11,13] According to Gibbs *et al.*,^[13] the activation energy for impurity diffusion of Ti in Mo is 180 kJ/mol, and Askill and Gibbs^[11] reported it to be 154 kJ/mol at temperatures less than 1473 K. The value for activation energy (172 kJ/mol) is quite comparable with these reported values. Similarly, the values for D_0 from the present experiments are of the same order as those reported by other workers, *i.e.*, 7×10^{-8} m²/s by Askill and Gibbs^[11] and 8×10^{-7} m²/s by Gibbs *et al.*^[13]

A similar approach to determine the impurity diffusion coefficient of Ti in Mo by Hall's method could not be attempted on the Mo-rich side of the concentration profile because of very steep slope. The concentration of Mo falls almost abruptly, and as the steps of measurement of concentration in an electron microprobe are limited to 1 μ m, enough data points could not be obtained for determining accurate values of D_{Ti}^{Mo} .

H. Inter-Relation between the Interdiffusion Parameters

The diffusion behavior in a particular system is expressed essentially by the two important parameters: the activation energy Q and the frequency factor D_0 . It has been shown by Zener^[14] and Swalin^[15] that the internal consistency of the two parameters requires a linear relation between $\ln D_0$ and Q . A similar relation was also put forward by Peleg^[16] for impurity diffusion. Such a linear relation between $\ln D_0$ and Q was also established by Kale^[17] for interdiffusion coefficients.

The values of $\ln D_0$ and Q for the interdiffusion coefficients at various compositions for the present system of Ti-Mo are plotted in Figure 12. The data points were fitted to a straight line by the least-squares method. The interrelation between $\ln D_0$ and Q can be expressed as

$$\ln D_0 = a + bQ. \quad [12]$$

The values of $a = -25.53$ and $b = 0.0526$ were determined from the equation of the linear regression line. These values are compared with those calculated for other systems such as Ti-V,^[17] Fe-V,^[18] Fe-Co,^[19] and Au-Ni^[20] in

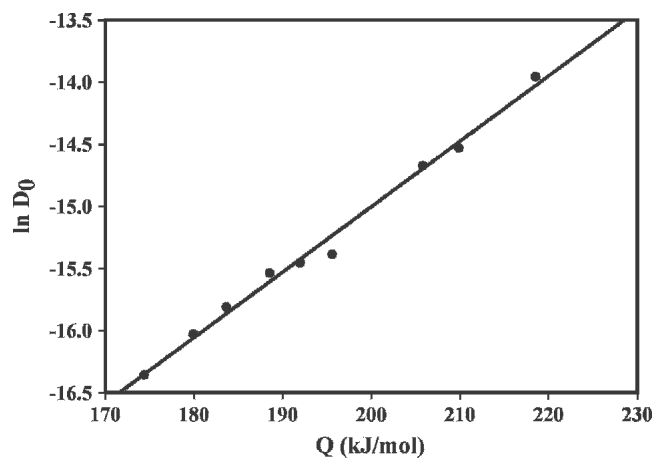


Fig. 12—Plot showing the linear dependence of the logarithmic values of the pre-exponential factor (D_0) with the activation energy (Q) for interdiffusion.

Table V. Values of the Constants a and b for the Relation $\ln D_0 = a + bQ$

System	Structure	$-a$	b	Reference
Ti-V	bcc	26.29	0.071	17
Fe-V	bcc	30.21	0.093	18
Ti-Mo	bcc	23.55	0.060	3
Ti-TZM	bcc	25.53	0.053	present study
Fe-Co	fcc	30.21	0.074	19
Au-Ni	fcc	30.21	0.093	20

Table V. The present values of the constants a and b match well with that calculated for the Ti-Mo system and with the other systems of bcc and fcc structures. Therefore, the diffusion mechanism in the present system may be the same as the other systems having bcc and fcc structures (Table V).

IV. CONCLUSIONS

1. The microstructure of the TZM base material consists of large elongated grains with precipitated carbide along the grain boundaries. The microstructure of the TZM/Ti shows excellent contact and the interface is devoid of any defects. The microstructure close to the interface shows retained β -(Ti, Mo) solid solution and the parent Ti shows sharp α' -Ti martensite plate structure.
2. The Ti and TZM were found to be mutually soluble in the β -(Ti, Mo) region. The nature of the concentration profiles across the TZM-Ti interface is like the systems having complete solubility in each other.
3. The concentration profiles are asymmetric about the MI. The Mo was found to migrate a large distance of about 50 to 80 μ m into Ti. However, Ti does not diffuse much into Mo on annealing in the range 1273 to 1373 K.
4. The kinetics parameters of diffusion were calculated at 1273 K. The values of the reaction index $n = 1.988$ and that of the penetration constant $k = 4.23 \times 10^{-7}$ ms^{-0.503}.
5. The interdiffusion coefficients, calculated using the Boltzmann–Matano method, were found to increase with the increase in the Ti concentration. This result is

consistent with the empirical rule that the diffusivity is a function of the solidus temperature. In the present case, diffusivity follows the solidus of the Mo-Ti binary system.

6. The activation energy for interdiffusion could be related to the concentration of Ti by a quadratic relationship, and the pre-exponential factor follows a linear relationship.
7. The impurity diffusion coefficient of Mo in Ti was calculated by extrapolation of the interdiffusion coefficient to infinite dilution. The results were found to be in agreement with the values reported earlier. The D_0 and Q values for impurity diffusion of Mo in Ti are $3.248 \times 10^{-7} \text{ m}^2/\text{s}$ and 171.98 kJ/mol, respectively.

ACKNOWLEDGMENTS

The authors are grateful to Dr. G.K. Dey, Head, Physical Metallurgy Section, Materials Science Division, and Shri B. P. Sharma, Associate Director (S), Materials Group, Bhabha Atomic Research Centre, for their keen interest in this work.

REFERENCES

1. A. Kohyama and S. Tanaka: *Proceedings of Japan/China Symposium on Materials for Advanced Energy Systems and Fission and Fusion Engineering '94*, Tokyo, 5-8 June 1994, H. Matsui and H. Takashahi, eds., 1994, pp. 222-28.
2. C.H. Caden and B.C. Odegard, Jr.: *J. Nucl. Mater.*, 2000, vols. 283-287, pp. 1253-57.
3. G.B. Kale and R.V. Patil: *Mater. Trans., JIM*, 1994, vol. 35, pp. 439-44.
4. I. Thibon, D. Ansel, M. Boliveau, and J. Debuigne: *Z. Metallkd.*, 1998, vol. 89, pp. 187-91.
5. J.L. Pouchou and F. Pichoir: *Microbeam Analysis*, San Francisco Press, San Francisco, CA, 1985.
6. C. Matano: *Jpn. J. Phys.*, 1933, vol. 8, pp. 109-13.
7. L. Boltzmann: *Annal. Phys.*, 1894, vol. 53, pp. 959-64.
8. A.D. Le Claire: *Progr. Met. Phys.*, 1949, vol. 1, pp. 306-79.
9. F.J. Gurney: Master's Thesis, Air Force Institute of Technology, OH, 1964.
10. L.D. Hall: *J. Chem. Phys.*, 1953, vol. 21, pp. 87-89.
11. J. Askill and G.B. Gibbs: *Phys. Status Solidi*, 1965, vol. 11, pp. 557-65.
12. H. Onodera, H. Ohyama, H. Nakajima, H. Takatori, H. Fujita, T. Maeda, H. Takahashi, and S. Watakabe: *Def. Diffus. Forum*, 1993, vols. 95-98, pp. 729-35.
13. G.B. Gibbs, D. Graham, and D.H. Tomlin: *Phil. Mag.*, 1963, vol. 8, pp. 1269-82.
14. C. Zener: *J. Appl. Phys.*, 1951, vol. 22, pp. 372-75.
15. R.A. Swalin: *J. Appl. Phys.*, 1956, vol. 27, pp. 554-55.
16. J. Pelleg: *Acta Met.*, 1966, vol. 14, pp. 229-31.
17. G.B. Kale: M.Sc. (Tech.), University of Bombay, Bombay, 1979.
18. R.E. Hanneman, R.E. Ogilvie, and H.C. Gatos: *Trans. AIME*, 1965, vol. 233, pp. 691-98.
19. K. Hirano, Y. Iijima, K. Araki, and H. Homma: *Trans. Iron Steel Inst. Jpn.*, 1977, vol. 17, pp. 194-99.
20. J.E. Reynolds, B.L. Averbach, and M. Cohen: *Acta Metall.*, 1957, vol. 5, pp. 29-40.